CHANNEL ESTIMATION AND EQUALIZATION FOR FBMC SYSTEMS

A Project Report

submitted by

POKALA VENKATA SUBBA REDDY

in partial fulfilment of the requirements

for the award of the degree of

MASTER OF TECHNOLOGY

Under the guidance of

Prof. R David Koilpillai

DEPARTMENT OF ELECTRICAL ENGINEERING
INDIAN INSTITUTE OF TECHNOLOGY MADRAS.

MAY 2016

THESIS CERTIFICATE

This is to certify that the thesis titled **CHANNEL ESTIMATION AND EQUALIZATION FOR FBMC SYSTEMS**, submitted by **POKALA VENKATA SUBBA REDDY**, to the Indian Institute of Technology, Madras, for the award of the degree of **Master of Technology**, is a bonafide record of the research work done by him under my supervision. The contents of this thesis, in full or in parts, have not been submitted to any other Institute or University for the award of any degree or diploma.

Prof.R David Koilpillai
Research Guide
Professor
Dept. of Electrical Engineering
IIT-Madras, 600 036

Place: Chennai

Date: 15^{th} May 2016

ACKNOWLEDGEMENTS

I would like to express my greatest gratitude for the people who have helped and supported me throughout my project. I am grateful to my guide, Prof. R David Koilpillai, for his continuous support. This project would not have been a success without his valuable suggestions and insights.

I would like to thank all the faculties in the Department of Electrical Engineering for teaching me with such patience which has helped me during my project work and in my studies.

I would like to thank my family, I am indebted to them forever for their never ending support and for giving me the freedom to make the decisions in my life.

Finally I would like to thank all my friends without whom my life would not be memorable.

ABSTRACT

KEYWORDS: OFDM , FBMC, PHYDYAS,OQAM,FC-FB .

This project gives an overview of some outcomes produced in the FP7 project PHYDYAS-PHYsical layer for DYnamic AccesS and cognitive radio. The main concern of the project is to analyze physical layer succeeding OFDM,i.e., a multi carrier system applying filter banks omitting severe out-of-band leakage of OFDM.First standard Filter bank structure was considered and reduced to another structure with polyphase elements of the prototype filter.Under this context performance comparison was made between FBMC and OFDM systems in spectrum,AWGN channel and Rayleigh channel. Different Equalizers along with their performance were studied with respect to polyphase designs.

Fast convolution(FC) implementation of Filter bank waveforms FBMC/OQAM(or OFDM/OQAM) was investigated. The generated waveforms are spectrally well contained, with very small power leakage to adjacent frequencies, and are thus good candidates for opportunistic and heterogenous spectrum use scenarios. On the receiver side FC Filter bank approach can be used for simultaneously processing multiple channels with individually tunable bandwidths,center frequencies supporting asynchronous multi-user operation. FC-FB implementations are compared with traditional polyphase designs in terms of spectral characteristics and performance over rayleigh channel.

TABLE OF CONTENTS

LIST OF TABLES

LIST OF FIGURES

ABBREVIATIONS

OFDM	Orthogonal Frequency Division Multiplexing
FBMC	Filter Bank MultiCarrier
AWGN	Additive White Gaussian Noise
OQAM	Offset Quadrature Amplitude Modulation
MCM	Multi Carrier Modulation
PPN	Poly Phase Network
SFB	Synthesis Filter Bank
AFB	Analysis Filter Bank
FIR	Finite Impulse Response
IIR	Infinite Impulse Response
NPR	Nearly Perfect Reconstruction
TMUX	TransMultiplexer
FFT	Fast Fourier Transform
IFFT	Inverse Fast Fourier Transform
ZF	Zero Forcing
MSE	Mean Square Error
PoP	Pair of Pilots
FC	Fast Convolution
RRC	Root Raised Cosine

CHAPTER 1

INTRODUCTION

Orthogonal frequency division multiplexing(OFDM) has been probably the most successful multi-carrier modulation(MCM) scheme for the wired or wireless communication in the past two decades and it is employed in the standard of today's 4G network. Meanwhile, OFDM still plays an important role in many current applications such as asymmetric digital subscriber line(ADSL), digital video broadcasting(DVB) and wireless local area networks (WLANs). However with increasing number of users and devices, the need for energy efficiency and sophisticated spectrum utilization at low costs drawbacks of OFDM become apparent such as the cyclic prefix(CP) leading to a decrease in the system efficiency. Consequently, other MCM methods have been proposed and evaluated recently and latest research indicates a great potential for these methods which may have a big influence on next generation communication systems and may replace the conventional OFDM.

One important, new emerging MCM method is the filter bank based multicarrier (FBMC) transmission, which introduces filter banks to the OFDM system and discards the CP. The employed filter bank will import extract flexibility to the system to cope with some drawbacks of OFDM. Intuitively, the filter bank can be designed with different properties to satisfy the communication requirements. For example, for the OFDM system, CP is used to eliminate inter symbol interference (ISI). In order to remove this interference completely, the length of CP must be no shorter than the length of the impulse response of the corresponding channel. However, this CP-redundancy decreases both spectral and power efficiency. For the FBMC, instead of CP, filter banks can be designed and applied to reduce the out-of-band power leakage and increase the spectral efficiency with a cost of computational complexity.

The outline of this project is as foloows. Chapter 2 discusses about polyphase approach to filter bank systems. Chapter 3 describes equalization and channel estimation techniques for Filter bank syatems. Implentation wise different structure Fast-convolution filterbank strucure was discussed in chapter 4. Simulation results are presented in chapter 5 and finally conclusions are drawn in chapter 6.

CHAPTER 2

FILTER BANK SYSTEM-POLYPHASE APPROACH

The principle of transmission based on filter banks is shown in Fig. 2.1. The transmitter contains a synthesis filter bank (SFB) and the receiver contains an analysis filter bank (AFB). In the structure of the figure, the FFT (Fast Fourier Transform) is present as in OFDM. It is augmented, to complete a filter bank, by the PPN (Polyphase Network) which consists of a set of digital filters, whose coefficients, globally, form the impulse response of the so-called prototype low-pass filter.

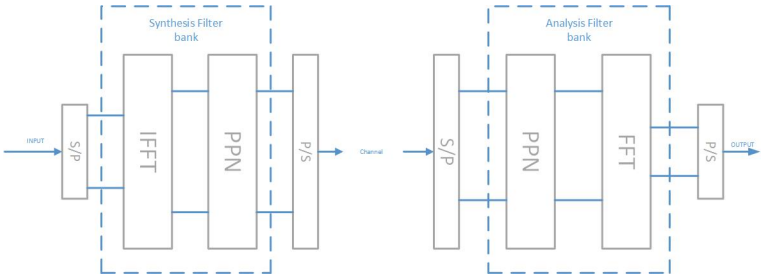

Figure 2.1: Filter Bank based Multi-carrier(FBMC) system

The essential difference between FBMC and OFDM resides in the frequency selectivity. This is illustrated in Fig. 2.2, which shows the frequency responses, around a particular sub-carrier, in both cases. OFDM exhibits large ripples in the frequency domain, which imposes the orthogonality constraint between all the sub-carriers. On the contrary, the filter bank frequency response has a negligible amplitude beyond the center frequency of the adjacent sub-carriers. In fact, the filter bank divides the transmission channel of the system into a set of sub-channels and any sub-channel overlaps with its immediate neighbors only. Then, in order to make two groups of contiguous subchannels independent, it is sufficient to leave a single empty subchannel between them.

The difference in frequency responses between FBMC and OFDM shown in Fig. 2.2 has a considerable impact on the performance of wireless systems and their operational flexibility. The FBMC approach has the following features:

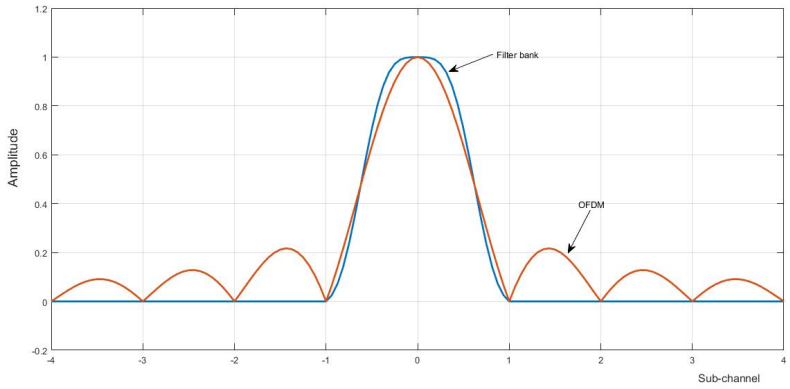

Figure 2.2: Comparison of frequency responses of OFDM and FBMC

- no guard time, or cyclic prefix, is needed

- full capacity of the transmission bandwidth is achieved using OQAM (Offset Quadrature Amplitude Modulation)

- frequency mask constraints for the transmitted signals are easily satisfied

- sub-channels can be grouped into independent blocks, which is crucial for scalability and dynamic access

- with the absence of leakage in the frequency domain, high resolution spectral analysis is achieved

- the same device can be used in cognitive radio for spectrum sensing and reception, even simultaneously, which guaranties perfect coherence between the two functions

2.1 Description of TMUX system

The TMUX configuration of FBMC system is shown in Fig. 2.3. The main processing blocks in the direct form representation are OQAM pre-processing, synthesis filter bank, analysis filter bank, and OQAM post-processing. The transmission channel typically omitted when analyzing and designing TMUX systems because the channel equalization problem is handled separately.

The synthesis and analysis filter banks are naturally the key components.The field of filter banks is very broad and even modulated filter banks can be divided into different types depending on the choice of the prototype filters, modulation functions, and desired properties. In this project, I have decided to study subchannel filter banks that

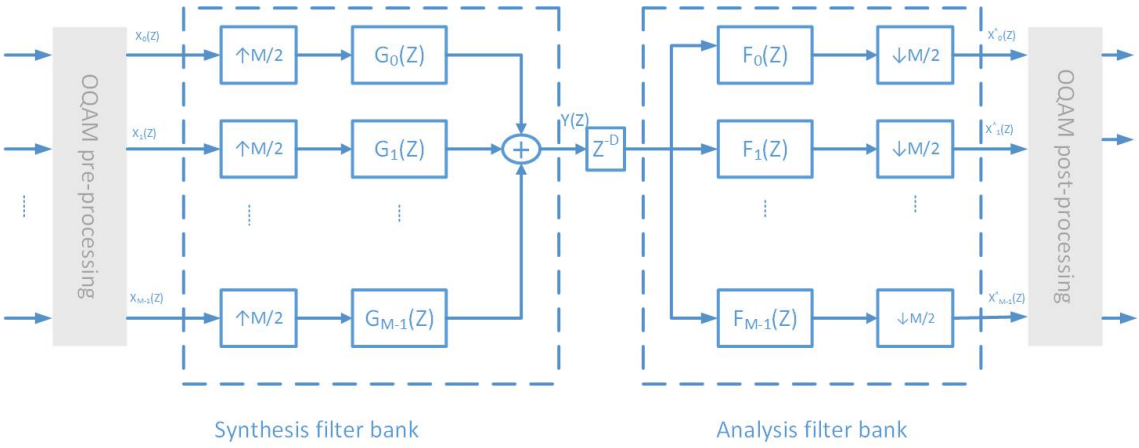

Figure 2.3: TMUX configuration

can be classified by the following terms:

- Complex modulated: In order to achieve a good spectral efficiency, a complex I/Q baseband signal is needed for transmission purposes and complex modulated filter banks are a logical choice. This means that all subchannel filters are frequency shifted versions of the prototype filter.
- Uniform: All subchannel filters have the same bandwidth as the prototype filter and they divide the available channel bandwidth equally.
- Finite impulse response (FIR): FIR filter banks are used instead of their infinite impulse response (IIR) counterparts because FIR filters are always stable and they are relatively easy to design and implement.
- Orthogonal: For orthogonal filter banks, only a single prototype filter is needed. Typically, linear-phase prototype filters are used, and therefore exponential modulation schemes can provide linear-phase subchannel filters. The resulting overall system delay depends on the order of the prototype filter.
- Nearly perfect reconstruction (NPR): The output signals are only approximately delayed versions of the input signals, i.e., certain amount of filter bank structure based distortions can be tolerated as long as they are small compared to those caused by a transmission channel.

The main filter bank design parameters are:

- The number of subchannels *M* is basically an arbitrary even number, but typically it is a power of two in order to provide efficient implementation.
- The most interesting filter lengths are chosen to be $L_p = KM - 1, L_p = KM$, and $L_p = KM + 1$, where *K* is a positive integer called as overlapping factor and it is selected to be 3 or higher.
- The prototype filter is designed in such a manner that only immediately adjacent subchannel filters are significantly overlapping with each other in the frequency domain.

The number of subchannels is twice the upsampling and downsampling factors indicating 2x oversampled filter banks if input and output signals are complex-valued. However, if input and output signals are purely real/imaginary-valued then the presented TMUX is equivalent to a critically sampled TMUX. This is because the sample rate (counted in terms of real-valued samples) of the SFB output and AFB input is equal to the sum of the sample rates of the subchannel signals. An extra delay Z^{-D}, with D depending on the length of the prototype filter ($L_p = KM + 1 - D$), has to be included either to the SFB ouput of AFB input.

2.1.1 OQAM pre/post-processing

Our TMUX system transmits OQAM symbols instead of QAM symbols. The pre-processing block, which utilizes the transformation between QAM and OQAM symbols, is shown in Fig. 2.4 As can be seen, the first operation is a simple complex-to-real conversion, where the real and imaginary parts of a complex-valued symbol $c_{k,l}$ are seperated to form two new symbols $d_{k,2l}$ and $d_{k,2l+1}$(this operation can also be called as staggering). The order of these new symbols depends on the subchannel number, i.e., the conversion is different for even and odd numbered subchannels. The complex-to-real conversion increases the sample rate by a factor of 2. The second operation is the multiplication by $\theta_{k,n}$ sequence.
A possible choice is

$$\theta_{k,n} = j^{(k+n)} \tag{2.1}$$

However, it should be noted that the signs of the $\theta_{k,n}$ sequence can be chosen arbitarily, but the pattern of real and imaginary samples has to follow the above definition. For example, an alternative sequence

$$\theta_{k,n} = \begin{cases} 1, j, 1, j, ... & \text{for } k \text{ even} \\ j, 1, j, 1, ... & \text{for } k \text{ odd} \end{cases} \tag{2.2}$$

can be used. Anyway, input signals are purely real or imaginary valued after the OQAM pre-processing.
The post-processing block is shown in Fig. 2.5 and again there are two slightly different structures depending on the subchannel number The first operation is the multiplication

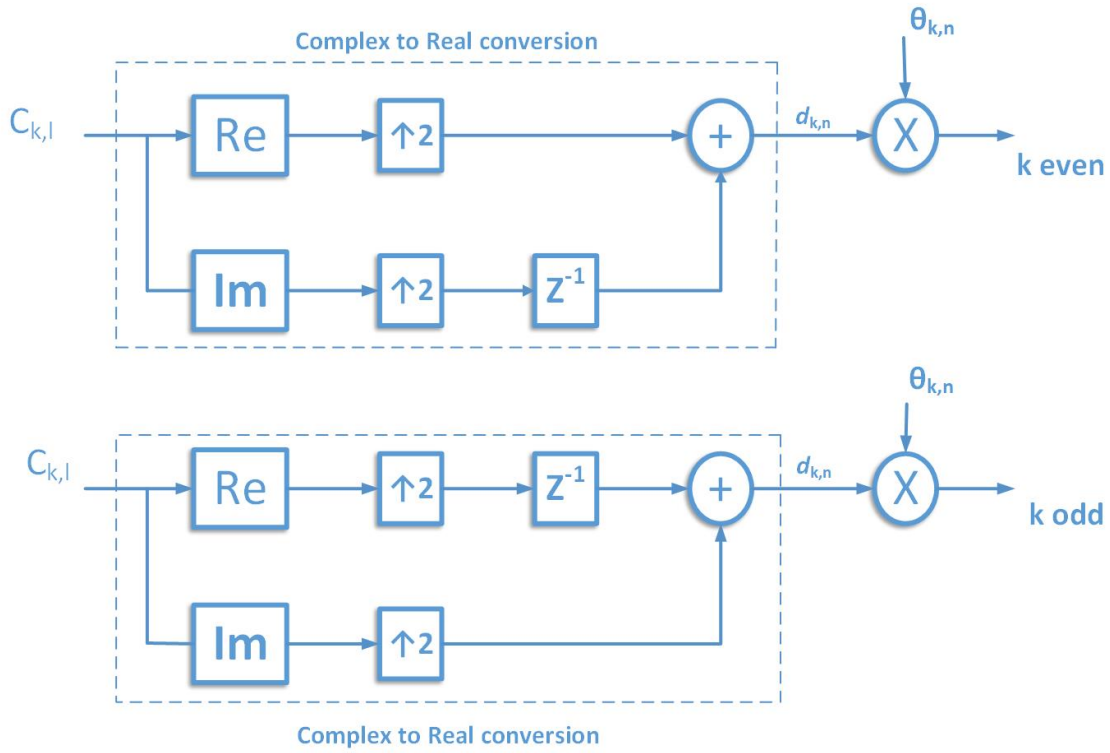

Figure 2.4: OQAM pre-processing section

by $\theta^*_{k,n}$ sequence that is followed by the operation of taking the real part. The second operation is real to complex conversion, in which two successive real-valued symbols (with one multiplied by j) form a complex-valued symbol $\hat{c}_{k,n}$(this operation is also called de-staggering). The real-to-complex conversion decreases the sample rate by a factor 2.

As can be seen, the first operation is a simple complex-to-real conversion, where the real and imaginary parts of a complex-valued symbol $c_{k,l}$ are separated to form two new symbols $d_{k,2l}$ and $d_{k,2l+1}$. The order of these new symbols depends on the subchannel number, i.e., the conversion is different for even and odd numbered subchannels. The complex-to-real conversion increases the sample rate by a factor of 2. The second operation is the multiplication by $\theta_{k,n}$ sequence

2.1.2 Synthesis and analysis filter banks

A direct form SFB consists of upsamplers and synthesis filters. As shown in Fig. 2.3, the input signals $X_k(Z)$ where $k = 0, 1, ..., M-1$, are first upsampled by $M/2$ and then filtered with synthesis filters $G_k(Z)$. The SFB output signal $Y(Z)$ is formed when

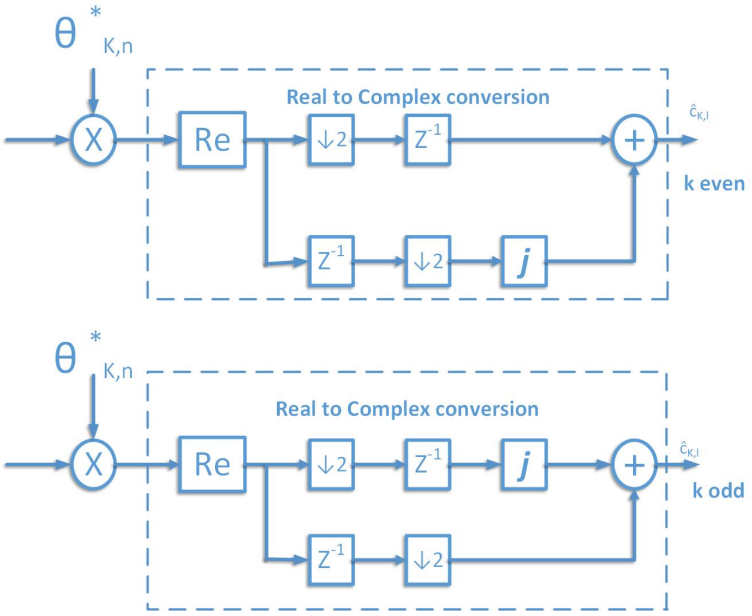

Figure 2.5: OQAM post-processing section

all subsignals are added together. A direct form AFB is constructed using M analysis filters and downsamplers as shown Fig. 2.3. The input signal signal Y(Z) is first filtered by analysis filters $F_k(Z)$ and these signals are downsampled by a factor of M/2 to form output signals $\hat{X}_k(Z)$.

In the case of chosen class of complex modulated filter banks, all subchannel filters can be generated from a single real-valued linear-phase lowpass prototype filter p[m] by using exponential modulation. Due to the modulation function, the resulting subchannel filters are complex-valued and therefore the useful frequency range is $[-\pi, \pi]$. Typically, two different types of channel stacking arrangements can be considered, namely, even-stacked filter banks and odd-stacked filter banks. The center frequencies of the k^{th} subchannel filters are $\omega_k = \frac{2k\pi}{M}$ and $\omega_k = \frac{(2k+1)\pi}{M}$ for even stacked and odd stacked filter banks, respectively.

In this project, even stacked filter banks are chosen. The k^{th} synthesis filter is defined by

$$g_k[m] = p[m]exp(j\frac{2\pi k}{M}(m - \frac{L_p - 1}{2})) \tag{2.3}$$

where m=0,1,...,$L_p - 1$ and L_p is the filter length. The k^{th} analysis filter is simply a

time-reversed and complex-conjugated version of the corresponding synthesis filter

$$\begin{aligned} f_k[m] &= g_k^*[L_p - 1 - m] \\ &= p[L_p - 1 - m]exp(-j\frac{2\pi k}{M}(L_p - 1 - m - \frac{L_p - 1}{2})) \\ &= p[m]\exp(j\frac{2\pi k}{M}(m - \frac{L_p - 1}{2})) \end{aligned} \tag{2.4}$$

An interpretation to the above equations is that first zero-phase subchannel filters are generated from a linear-phase prototype filter and then their impulse responses are delayed by $\frac{L_p-1}{2}$ samples resulting in causal subchannel filters. Due to nature of the modulation function the 0^{th} subchannel filter is purely real and $\frac{M}{2}^{th}$ is purely imaginary. However all subchannel filters have linear phase.

2.2 Efficient implementations of filterbank structures

The direct form implementations of Fig. 2.3 are not very efficient for practical applications because filtering operations are performed at the high sampling rate leading to huge amount of unnecessary calculations. So Polyphase structures which is one of efficient multirate structure was used. Polyphase structures consist of filter section, the coefficients of which are determined by the prototype filter and the transform section implementing the modulation.The polyphase structures are the only ones that can be applied to NPR filter banks. Their main advantage is that they can offer drastic simplifications because filtering operations are done at the lower sampling rate and no unnecessary calculations are performed. Next, polyphase structures for SFBs and AFBs are derived.

2.2.1 Polyphase structure of synthesis filter bank

In the case of modulated filter banks, the number of the polyphase filter branches depends on the periodicity of the modulation function. The periodicity of modulation

function used in synthesis and analysis filters.i.e.,

$$\begin{aligned} e_{k,m} &= \exp(j\frac{2\pi k}{M}(m - \frac{L_p - 1}{2})) \\ &= \exp(-j\frac{2\pi k}{M}(\frac{L_p - 1}{2})\exp(j\frac{2\pi km}{M}) \\ &= \beta_k \Theta_{k,m} \end{aligned} \tag{2.5}$$

M because $\Theta_{k,q+tM} = \Theta_{k,q}$, where $q = 0, 1, .., M-1$ and $t = 0, 1, .., K-1$. Now the k^{th} synthesis filter can be expressed in the form of type-1 polyphase filters as foloows.

$$\begin{aligned} G_k(z) &= \sum_{m=0}^{L_p-1} p[m] e_{k,m} z^{-m} \\ &= \sum_{q=0}^{M-1} \sum_{t=0}^{K-1} p[q+tM] \beta_k \Theta_{k,q+tM} z^{-(q+tM)} \\ &= \sum_{q=0}^{M-1} \beta_k \Theta_{k,q} z^{-q} \sum_{t=0}^{K-1} p[q+tM] z^{-tM} \\ &= \sum_{q=0}^{M-1} \beta_k \Theta_{k,q} z^{-q} A_q(z^m) \end{aligned} \tag{2.6}$$

Now all synthesis filters can be compactly represented using the following matrix notation

$$G(z) = B \cdot W \cdot A(Z^M) \cdot c(Z) \tag{2.7}$$

where

$$\begin{aligned} G(z) &= [G_0(z) G_1(z) ... G_{M-1}(z)]^T, \\ B &= diag[\beta_0 \beta_1 ... \beta | M-1], \\ [W]_{k,q} &= \Theta_{k,q}, \\ A(z^M) &= diag[A_0(z^M) A_1(z^M) ... A_{M-1}(z^M)] \\ c(z) &= [1 z ... z^{-(M-1)}]^T \end{aligned} \tag{2.8}$$

The starting point of polyphase structure is the direct form synthesis filter bank shown in Fig. 2.1. The output signals without downsampling can be written using matrix

notations as

$$\begin{aligned} Y(z) &= G^T(z) \cdot X(z^{M/2}) \\ &= (B \cdot W \cdot A(z^M)c(z))^T X(z^{M/2}) \\ &= c^T(z) \cdot A(z^M) \cdot W \cdot B \cdot X(Z^{M/2}) \end{aligned} \tag{2.9}$$

where $X(z^{M/2}) = [X_0(z^{M/2})X_1(z^{M/2})...X_{M-1}(z^{M/2})]^T$. The above equation can be interpreted in such a manner that the synthesis filter bank consists of upsamplers by $M/2$, β_k-multipliers, IDFT, type-1 polyphase filters $A_q(z^M)$, and delay chain. By using multirate identities all upsamplers can be moved through β_k -multipliers IDFT, and polyphase filters. The resulting polyphase implementation structure is shown in Fig. 2.6. It can be noticed that upsamplers and delay chain form a parallel-to-serial(P/S) converter with overlapping of $M/2$. This is because the number of branches is M and the upsampling factor is only M/2. In this sense, $A_k(z^2)$ and $A_{k+M}(z^2)$ could actually share a common delay line.

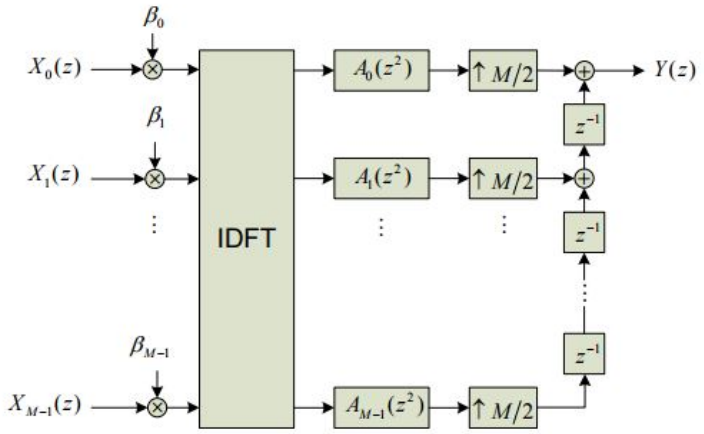

Figure 2.6: polyphase implementation of synthesis filterbank

2.2.2 polyphase structure of analysis filter bank

The analysis filters are defined using exactly the same equation as the synthesis filters. Therefore, the polyphase decomposition of the k^{th} analysis filter bank can be directly written as follows

$$\begin{aligned} F_k(z) &= \sum_{m=0}^{L_p-1} h_p[m] e_{k,m} z^{-m} \\ &= \sum_{q=0}^{L_p-1} \beta_k \Theta_{k,q} z^{-q} A_q(z^M) \end{aligned} \tag{2.10}$$

Moreover, all analysis filters can be written using the matrix notation as follows

$$F(z) = B \cdot W \cdot A(z^M) \cdot c(z) \tag{2.11}$$

where

$$F(z) = [F_0(z)F_1(z)...F_{M-1}(z)]^T. \tag{2.12}$$

The starting point of polyphase structure is the direct form analysis filter bank shown in Fig. 2.7.The output signals can be written using matrix notations as

$$\begin{aligned} \hat{X}(z^{M/2}) &= F(z^M) \cdot Y(z) \\ &= B \cdot W \cdot A(z^M) \cdot c(z) \cdot Y(z) \end{aligned} \tag{2.13}$$

where $\hat{X}^(z^{M/2}) = [\hat{X}_0(z^{M/2})\hat{X}_1(z^{M/2})...\hat{X}_{M-1}(z^{M/2})]^T$. The analysis filter bank can be interpreted to consist of delay chain, type-1 polyphase filters, IDFT, β_k-multipliers, and downsamplers by $M/2$. The downsamplers by $M/2$ can be moved through β_k-multipliers, IDFT, and polyphase filters. The resulting polyphase implementation structure is very similar to synthesis filters. The same main processing blocks as in the case of synthesis filter bank are used but in reverese order.

It can be noticed that delay chain and downsamplers form an serial-to-parallel con-

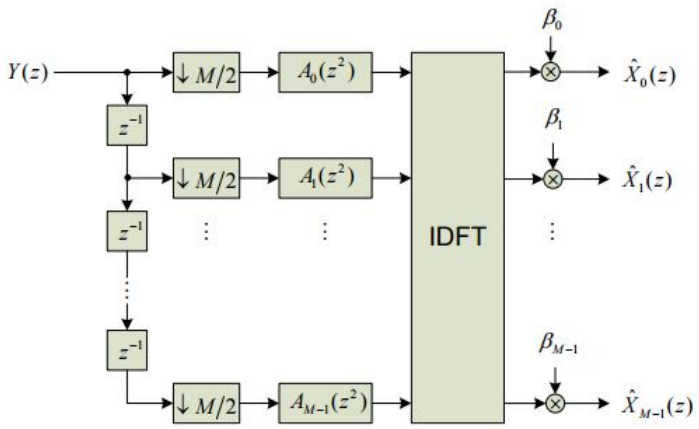

Figure 2.7: polyphase implementation of analysis filterbank

verter(S/P) with overlapping of $M/2$. Again this means that polyphase filters $A_q(z^2)$

and $A_{k+qM}(z^2)$ could actually share a common delay line.

2.3 Prototype filter

The prototype filter is a key element in the complex modulated filter banks because all synthesis and analysis filters are frequency shifted versions of the corresponding low-pass prototype filter frequency response. In this sense, the quality of filter bank system depends mainly on the properties of the prototype filter.In this project, the prototype filter is selected to be a causal real valued symmetric FIR filter with high frequency selectivity.

Frequency sampling based design of prototype filter

There exist plenty of different techniques to design complex modulated filter banks. In this project, A simple technique to design the prototype filter is the so-called frequency sampling technique was considered with the following parameters.

$$L_p = 2048; M = 512; K = 4$$

The design starts with the determination of L_p desired values $H(k/L_p); 0 \leq k \leq L_p - 1$ in the frequency domain by

$$\begin{aligned} H(0) &= 1 \\ H(1/L_p) &= 0.97196 \\ H(2/L_p) &= 1/\sqrt{2} \\ H(3/L_p) &= \sqrt{1 - H^2(1/L_p)} \\ H(k/L_p) &= 0; 4 \leq k \leq L_p - 1 \end{aligned} \tag{2.14}$$

Then, the prototype filter coefficients are obtained by inverse DFT as

$$p[m] = 1 + 2\sum_{k=1}^{K-1}(-1)^k H(k/L_p)\cos(2\pi km/L)$$
$$p[0] = 0 \tag{2.15}$$

In fact, the condition $p[0] = 0$ determines the desired values $H(1/L_p)$ and $H(3/L_p)$. It is useful to make the number of coefficients an odd number, in which case the filter delay can be adjusted to be an integer number of sample periods.

The frequency response obtained is shown in Fig. 2.8 . In this figure, the sub-channel spacing Δf is taken as unity. It is important to notice that the filter attenuation exceeds 60dB for the frequency range above 2 sub-channel spacings.

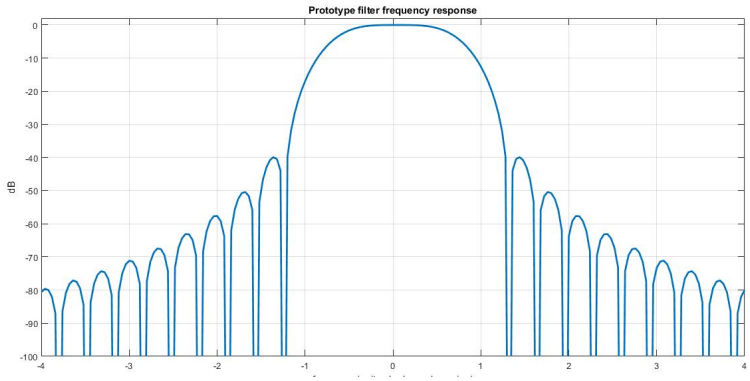

Figure 2.8: Frequency response of prototype filter

2.4 Transmultiplexer response

The transmultiplexer response, $t_{k,n}$ is determined by the filter bank design. The transmultiplexer response of the reference filter bank system is illustrated in Table. 2.1

sub-ch \time	-4	-3	-2	-1	0	1	2	3	4
-2	0	0.0006	-0.0001	0	0	0	-0.0001	0.0006	0
-1	0.0054	j0.0429	-0.1250	-j0.2058	0.2393	j0.2058	-0.1250	-j0.0429	0.0054
0	0	0.0668	0.0002	0.5644	1	0.5644	0.0002	0.0668	0
1	0.0054	-j0.0429	-0.1250	j0.2058	0.2393	-j0.2058	-0.1250	j0.0429	0.0054
2	0	0.0006	-0.0001	0	0	0	-0.0001	0.0006	0

Table 2.1: Transmultiplexer response of the FBMC system using PHYDYAS reference bank

It can be seen that the effect of subchannel k on the second adjacent subchannels $(k-2, k+2)$ is very small. In the time direction, the effect of sample at time n extends to the range $n-4$ to $n+4$, due to the overlapping factor of 4. The non-orthogonality (due to NPR design) can be seen in the samples $(k \pm 2, n \pm 2)$, $(k, n \pm 2)$, which are quite small in magnitude.

CHAPTER 3

CHANNEL ESTIMATION AND EQUALIZATION

In FBMC communications, the filter banks are used in the transmultiplexer(TMUX) configuration, with the synthesis filter bank(SFB) in the transmitter and the analysis filter bank(AFB) in the receiver. Fig. 3.1 shows the filter banks in this configuration as fundamental part of a complete FBMC/OQAM transmission/reception system. This FB technique builds on uniform modulated filter banks, in which a prototype filter $p[m]$ of length L_p is shifted in frequency to generate subbands which cover the whole system bandwidth. The output of such a synthesis filter bank can be expressed by

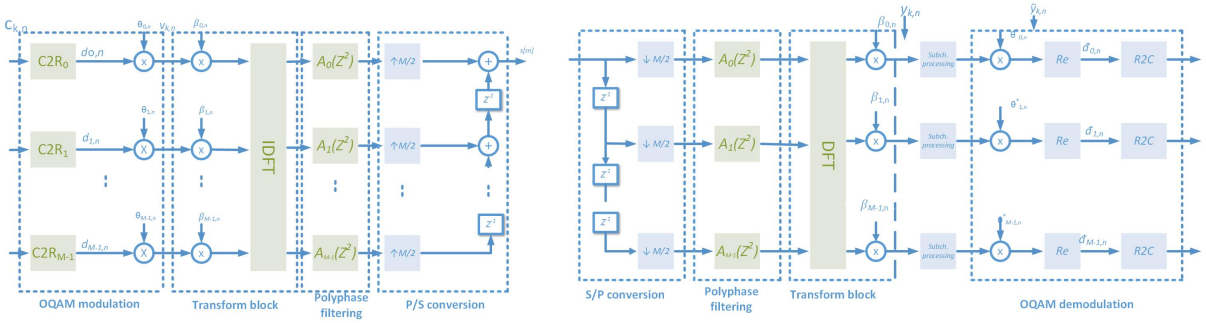

Figure 3.1: Synthesis and analysis filter banks for complex FBMC transmultiplexer(TMUX) with per-subchannel processing

$$s[m] = \sum_{k=0}^{M-1} \sum_{n=-\infty}^{\infty} d_{k,n}\theta_{k,n}p[m - \frac{nM}{2}]e^{j(2\pi/M)k(m-n(M/2)-((L_p-1)/2))} \tag{3.1}$$

where

$$\theta_{k,n} = e^{j(\pi/2)(k+n)} = j^{k+n} \tag{3.2}$$

m is the sample index at the output of SFB(at high rate),

M is the number of subchannels in the filter bank,

$d_{k,n}$ are the real-valued data symbols in subchannel *k*, transmitted at a rate $2/T$.

The signaling interval is defined as $T = 1/\Delta f$, where Δf is the subcarrier spacing.

The pair of symbols $d_{k,n}$ and $d_{k,n+1}$ can be interpreted as carrying the in-phase and

quadrature information of a complex valued symbol transmitted at rate $1/T$. Therefore, the filter bank presented in Fig. 3.1 is critically sampled. The "$C2R_k$" blocks indicate the conversion into real-valued data from the real and imaginary parts of the complex-valued input symbols $c_{k,n}$ and can be considered as introducing upsampling by 2. "R2Ck" carries out the inverse operation after the AFB in the receiver, effectively downsampling the signal by 2. In FBMC/OQAM, $c_{k,n}$ belongs to a QAM alphabet and the real and imaginary parts are interleaved with a relative time offset of $T/2$ (hence offset QAM) and $C2R_k$ performs the following mapping.

$$d_{k,2n} = \begin{cases} Re[c_{k,n}] & \text{for } k \text{ even} \\ im[c_{k,n}] & \text{for } k \text{ odd} \end{cases}$$
$$d_{k,2n+1} = \begin{cases} Im[c_{k,n}] & \text{for } k \text{ evem} \\ Re[c_{k,n}] & \text{for } k \text{ odd} \end{cases} \tag{3.3}$$

Note that the signs of the sequences in above equations could be chosen arbitrarily, but the pattern of real and imaginary symbols after multiplication by $\theta_{k,n}$ has to follow the above definitions to maintain orthogonality.

This type of filter bank pairs can be efficiently implemented using FFT and IFFT of size *M* aided by polyphase filtering structures. The different parts of the polyphase SFB structure of Fig. 3.1 can be better identified by noting that $a_k[m] = p[m + kM]$ and rewriting Eq. 3.1 as

$$s[m] = \sum_{k=0}^{M-1} \sum_{n=-\infty}^{\infty} d_{k,n}\theta_{k,n}\beta_{k,n}p[m - \frac{nM}{2}]e^{j(2\pi/M)km} \tag{3.4}$$

where

$$\beta_{k,n} = (-1)^{kn} \cdot e^{-j(2\pi k/M)((L_p-1)/2))} \tag{3.5}$$

here, the factor $(-1)^{kn}$centres the low-rate output signal ofeach suchannel *k* of the analysis filter bank around DC.

3.1 Equalization

Equalization is an essential part of the processing at the receiver, necessary to take care of the multipath nature of the transmission channel. One of the big advantages of FBMC is that it allows simple per-subcarrier equalization, just as in OFDM, without the loss of bandwidth efficiency associated with the cyclic prefix. FBMC relies on the selectivity of the filter bank filters to mitigate the intercarrier interference and ensures that each subcarrier is narrow enough to have a virtually flat channel inside its bandwidth. Several factors need to be considered regarding equalization issue. They are summarized below.

Number of subcarriers: It is necessary to choose a sufficient number of subcarriers, so that each individual subcarrier has a narrow bandwidth and can be equalized easily, with a limited number of taps. In addition, a high number of subcarriers provide a higher resolution in terms of spectrum sensing, and an increased versatility for frequency division among users for instance. On the downside, the complexity increases with the number of subcarriers, and the sensitivity to synchronization issue is also increased. The burst truncation effects are also more difficult to mitigate when using higher number of subcarriers.

OQAM demodulation: The particular format of the OQAM modulation, transmitting alternatively on the real and imaginary part, allows to take full advantage of the bandwidth and transmit at high bandwidth efficieny. Equalization needs however to make sure that no intersymbol is generated between the real and imaginary parts due to the channel frequency selectivity.

Fractional sampling: The symbol duration is here denoted by T. As the symbols are actually generated at $T/2$ due to the OQAM modulation format, it is natural for the equalizer to work at the fractional sampling $T/2$. It has the advantage of corresponding to the approximate bandwidth of each individual filter of the filter bank, which means that no aliasing is generated when performing the equalization at the fractional sampling. So equalizer considered in this project work at this rate.

Channel estimation: Most equalizer designs are based on the assumption that some channel estimate is available. It is thus necessary to investigate accurate channel estimation. Different methods using pilot symbols are presented in this project. It is of course necessary both to estimate the channel at the initialization, as well as track the

changes of the channel due to the mobility in a wireless environment.

In OFDM as long as the channel delay spread and the possible synchronization errors remain within the cyclic prefix time, equalization can be simply done with complex coefficient multiplication at subsubcarrier level. This approach is also applicable to FBMC, if the ratio of channel delay spread in samples and number of subchannels is sufficiently low, since the frequency variation within a subchannel is small enough that it can be considered flat fading. But as this is not the general case, more effective channel equalization methods have been developed for FBMC. A simple subchannel wise equalizer structure is discussed in this project. When it is needed to cope with very selective channels, the equalizer can be further improved by using a multi-band equalizer, as opposed to per-subcarrier equalizer. The idea is to use the outputs of the analysis filter bank corresponding to adjacent subcarriers instead of using only the output of the corresponding subcarrier, as these outputs also contain some useful power.

3.1.1 Complex FIR equalizer

The working principle is based on frequency sampling: assuming a roll-off factor of the prototype filter $\alpha = 1$ or smaller, each subchannel overlaps only with the immediately neighbouring subchannels. At the oversampled part of the receiver bank, before taking the real part of the subcarrier signals, the equalizer can perform equalization at a number of frequency points according to its complexity. Equalizer under consideration is 3-tap complex FIR filter, so 3 frequency points within the subchannel can be completely equalized, according to the zero-forcing (ZF) or the mean squared error (MSE) criterion. With the filter bank structure shown in the Fig. 3.1, all the subchannels alias to frequencies centered around DC, and a straightforward choice is to equalize at DC and at $\pm\pi/2$, that is, the center of the subchannel and the passband edge frequencies, respectively. Also other frequencies can be used, as well as longer filters.

3-tap equalizer:

Here, three frequency points are used for channel equalization. One frequency point is located at the center of the subchannel frequency band, at $\omega = \pm\pi/2$ and two frequency

points are located at the passband edges of the subchannel, at $\omega = 0$ and $\omega = \pm\pi$. Transfer function of 3-tap complex FIR equalizer of subchannel *k* at time *n* is

$$W_{k,n}(z) = w_{k,n}^{(-1)} z + w_{k,n}^{(0)} + w_{k,n}^{(1)} z^{-1} \tag{3.6}$$

the filter coefficients $w_{k,n}^{(d)}$, with *d*=-1,0,1 can be tuned in a way that the filter achieves the following target values at the mentioned frequency points.

$$\chi_{k,n}^{(i)} = \gamma \frac{(H_{k,n}^{(i)})^*}{|H_{k,n}^{(i)}|^2 + \xi} \tag{3.7}$$

Here $i \in \{0,1,2\}$,where i =0 corresponds to the lower subband edge, i =1 corresponds to the subband center, i =2 to the upper subband edge frequency. $H_{k,n}^{(i)}$ is the channel frequency response in subchannel *k* and time *n* at frequency position given by *i*, and γ and ξ are scaling factors. If the equalizer applies ZF criterion, ξ=0 and γ=1. In the MSE case, ξ is the noise to signal power ratio and the choice of

$$\gamma = \frac{3}{\sum_{i=0}^{2} (|H_{k,n}^{(i)}|^2 / (|H_{k,n}^{(i)}|^2 + \xi))} \tag{3.8}$$

removes the bias of MSE solution.

Taking into account these assumptions, the equalizer coefficients can be derived from the target values as.

$$\begin{aligned} w_{k,n}^{(-1)} &= \frac{-\chi_{k,n}^{(0)}(1-j) + 2\chi_{k,n}^{(1)} - \chi_{k,n}^{(2)}(1+j)}{4} \\ w_{k,n}^{(0)} &= \frac{\chi_{k,n}^{(0)} + \chi_{k,n}^{(2)}}{2} \\ w_{k,n}^{(1)} &= \frac{-\chi_{k,n}^{(0)}(1+j) + 2\chi_{k,n}^{(1)} - \chi_{k,n}^{(2)}(1-j)}{4} \end{aligned} \tag{3.9}$$

3.2 Channel estimation

In this section, channel estimation methods for FBMC systems are investigated. The focus is here mostly on data-aided methods, i.e., the channel estimation is based on known transmitted symbols, which may appear either in the form of preambles or pi-

lots. A preamble is a special multicarrier symbol, in the beginning of the transmission frame, which is designed for synchronization and channel estimation purposes and does not carry user data. In the multicarrier literature, pilots refer to known training symbols, which are scattered among data symbols at predetermined subcarrier symbol positions, following patterns which are characteristic to each particular system.

Due to the use of OQAM subcarrier modulation, the use of pilots in FBMC systems is not as straightforward as in OFDM. First signal model is considered to calculate interference from adjacent symbols and then pilot schemes are considered to reduce/approximate interference so that channel estimate is more accurate.

The baseband signal model at the receiver input with effect of linear multipath channel and AWGN can be expressed as

$$r(t) = s(t) * h(t, \tau) + \eta(t) \tag{3.10}$$

where * represents the convolution operation, s(t) is the continuous version of transmitted signal, $h(t, \tau)$ is the time varying transmission channel,$\eta(t)$ is complex valued AWGN. At the receiver, $r(t)$ is sampled at $T_s = T/M$ into $r[m]$ and then passes tha analysis bank. Before the subchannel processing stage, the k^{th} subchannel sequence $y_{k,n}$ can be expressed as

$$y_{k,n} = [r[m] * f_k[m]]_{\downarrow M/2} = \sum_{i=0}^{M-1} v_{i,n} * q_{i,k,n} + \eta_{k,n} \tag{3.11}$$

where

$$\begin{aligned} q_{i,k,n} &= [g_i[m] * h[n, m] * f_k[m]]_{\downarrow M/2} \\ v_{i,n} &= \theta_{i,n} d_{i,n} \end{aligned} \tag{3.12}$$

In an FB system with a sufficiently frequency selective prototype filter and roll-off $\alpha \leq 1$, only adjacent subchannels overlap and have an effect on subchannel *k* of interest. This implies

$$y_{k,n} = \sum_{i=k-1}^{k+1} v_{i,n} * q_{i,k,n} + \eta_{k,n} \tag{3.13}$$

$$
\begin{aligned}
y_{k,n} &= \sum_{i=k-1}^{k+1} \sum_{l=-\infty}^{\infty} v_{i,l} q_{i,k,n-1} + \eta_{k,n} \\
&= v_{k,n} + \sum_{i=k-1}^{k+1} \sum_{\substack{l=-\infty \\ (i,l)\neq(k,n)}}^{\infty} v_{i,l} q_{i,k,n-1} + \eta_{k,n}
\end{aligned}
\tag{3.14}
$$

equivalently, we can write

$$
\begin{aligned}
\tilde{y}_{k,n} &= \theta^*_{k,n} y_{k,n} \\
&= \theta^*_{k,n} v_{k,n} + \theta^*_{k,n} \sum_{i=k-1}^{k+1} \sum_{\substack{l=-\infty \\ (i,l)\neq(k,n)}}^{\infty} v_{i,l} q_{i,k,n-1} + \theta^*_{k,n} \eta_{k,n} \\
&= d_{k,n} + \sum_{i=k-1}^{k+1} \sum_{\substack{l=-\infty \\ (i,l)\neq(k,n)}}^{\infty} j^{i-k} d_{i,l} q_{i,k,n-l} + \theta^*_{k,n} \eta_{k,n} \\
&= d_{k,n} + (\eta^{NPR}_{k,n} + j u_{k,n}) + \theta^*_{k,n} \eta_{k,n}
\end{aligned}
\tag{3.15}
$$

The elements $\eta^{NPR}_{n,k}$ and $u_{k,n}$ within the paranthesis of above equation are obtained by respectively, taking real and imaginary parts of interference term in teh above equations. These are interference terms on the desired symbol $d_{k,n}$. In NPR designs, $\eta^{NPR}_{k,n}$ is a small real valued contribution, generally well below the level of $\eta_{k,n}$ and can be ignored. Another property of imaginary valued interference $ju_{k,n}$ is that it is time-varying, since it depends on the data in the adjacent channels and on the symbols preceding and following $d_{k,n}$.

For simplicity of notation, define the noncausal TMUX response at subchannel *k* and instant *n* as $t_{k,n}$. It is assumed that it is normalized at *k*=0 and *n*=0 as $t_{0,0} = 1$. Table. 2.1 presents the interference weights that multiply neighboring symbols in the case of an NPR prototype designed with PHYDYAS prototype filter and overlapping factor K=4. Thus, we obtain at the location (k_0, n_0) of interest

$$
\tilde{y}_{k_0,n_0} = \theta^*_{k_0,n_0} y_{k_0,n_0} = d_{k_0,n_0} + j u_{k_0,n_0} + \eta_{k_0,n_0} \tag{3.16}
$$

where the imaginary interference is

$$
u_{k_0,n_0} = \sum_{(k,n)\epsilon\Omega_{k_0,n_0}} d_{k,n} \hat{t}_{k_0-k,n_0-n} \tag{3.17}
$$

with

$$\hat{t}_{k,n} = Im[\theta^*_{k,n} t_{k,n}] \tag{3.18}$$

and Ω_{k_0,n_0} is the set of subcarrier and time indices that are considered to contribute to the interference on the symbol at (k_0, n_0). Without channel distortions *t* and *q* are related as $q_{i,k,n} = t_{k-i,n}$.

Table. 2.1 shows that the interference from subchannels not adjacent to the subchannel of interest have negiligible effect and that in time direction the interference goes K symbols from the symbol of interest in both directions. It is clear that pilot located at subcarrier K_p and time n_p cannot be immediately recovered even if the channel at that subcarrier is a simple complex coefficient H_{k_p,n_p}, because the pilot information and the complex valued, time varying and data dapendent interference will be mixed by the channel. Different pilot scemes are addressed below to cancel/approximate interference at the pilot location. Simulation results with these techniques are given in SIMULATION RESULTS chapter.

3.2.1 Auxiliary pilots

This approach is based on the idea of utilizing an auxiliary pilot located at k_a, n_a adjacently to the pilot k_p, n_p and which cancels the interference u_{k_p,n_p}. The advantage of eliminating the interference is that the pilots can be used at the receiver in a similar fashion as OFDM pilots are used; the estimate of the channel at the pilot location is

$$\hat{H}_{k_p,n_p} = \frac{\theta^*_{k_p,n_p} y_{k_p,n_p}}{d_{k_p,n_p}} \tag{3.19}$$

assuming that the channel is constant over the whole subchannel bandwidth. The auxiliary pilot is indeed one element of the sum Eq. 3.17 and has to be calculated online with data transmission every time a pilot is inserted since the interference terms vary with the data. The number of surrounding symbols chosen to cancel the interference depends on time-frequency localization of prototype filter. The auxiliary pilot that cancels the interference can be calculated as

$$d_{k_a,n_a} = -\frac{1}{\hat{t}_{k_p-k_a,n_p-n_a}} \sum_{\substack{(k,n)\epsilon\Omega_{k_p,n_p} \\ (k,n)\neq(k_p,n_p) \\ (k,n)\neq(k_a,n_a)}} d_{k,n}\hat{t}_{k_p-k,n_p-n} \tag{3.20}$$

In typical filter bank designs it is wise to locate the auxiliary pilot immediately preceding or following the pilot, that is, $n_a = n_p - 1$ or $n_a = n_p + 1$. This way, the absolute value of the denominator $\hat{t}_{k_p-k_a,n_p-n_a}$ is maximized and the magnitude of auxiliary pilot is minimized on the average wasting less transmission energy on the pilot/auxiliary pilot pair and preventing possible strong effects on the peak-to-average-power ratio (PAPR) due to excessively strong auxiliary pilots. In this project, three symols in time domain and one symbol in adjacent subcarrier on either side of the pilot are considered while calculating auxiliary pilot value.Note that the use of two real-valued symbols as pilots does not mean a penalty in overhead with respect to OFDM, since there the pilot is complex-valued.

3.2.2 Interference approximation method

This method is preamble based channel estimation technique and can be extended to scattered pilot estimation also. The philosophy here is that the most of the symbols surrounding the pilot in time and frequency are fixed and known at the receiver. The preamble used is shown below. In this case, the interference u_{k_p,n_p} can be approximately calculated with Eq. 3.17 which leads to the estimate

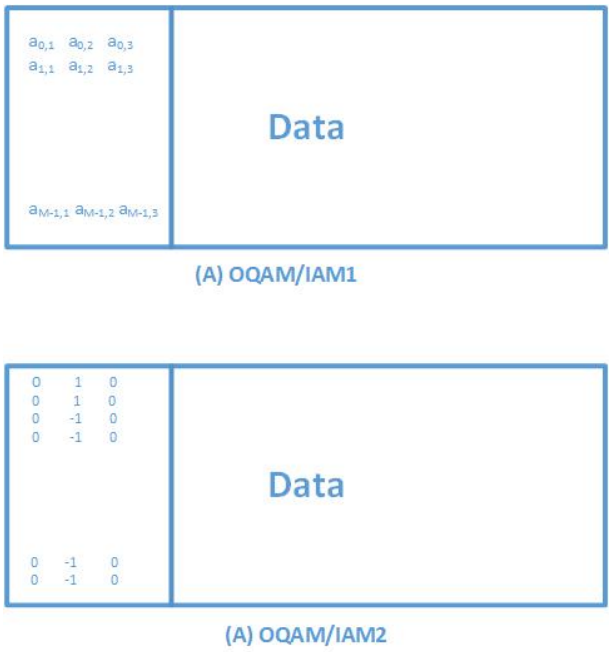

Figure 3.2: Preamble for OQAM/IAM method

$$\hat{H}_{k_p,n_p} = \frac{\theta^*_{k_p,n_p} y_{k_p,n_p}}{d_{k_p,n_p} + j u_{k_p,n_p}}. \tag{3.21}$$

The symbols around the pilot fixed , the better is the approximation of u_{k_p,n_p}. Unfortunately, this approach leads to an unacceptable overhead if a good approximation of the interference, necessary for accurate channel estimates, is desired. Therefore, it is practical only in situations in which pilots are packed closely together, for example, in preambles, where the fixed symbols can be simultaneously utilized by nearby located pilots.

3.2.3 Pair of Pilots method

The pair of real pilots (POP) method also uses two consecutive OQAM subsymbols to send known pilots, in the simplest case, similar pilots. Ignoring the noise and assuming that the channel remains unchanged during both subsymbols, an equation system yields the equalizer coefficient (the same for both pilots) that restores the pilots to their original phase. Its inverse is the estimate for the channel at the positions of the POP. This method places the computational complexity on the receiver part and has the advantage that it is independent from the prototype filter design, since the interference term is not used explicitly in the equations. However, if the noise is not negligible, it will be enhanced in a random fashion, depending on the data surrounding the pilots, which makes the performance unpredictable and generally worse. Preamble used for this technique is shown below.

Figure 3.3: Preamble for OQAM/POP method

Let $(k_1, n_1), (k_2, n_2)$ are two reference symbol positions and assume $y^{(c)}_{k,n}(\cdot) = \tilde{y}_{k,n}(\cdot)$, $(.)^{(c)}$ represents complex value] then we have

$$\begin{aligned} y^{(c)}_{k_1,n_1} &= H^{(c)}_{k_1,n_1}(d_{k_1,n_1} + ju_{k_1,n_1}) \\ y^{(c)}_{k_2,n_2} &= H^{(c)}_{k_2,n_2}(d_{k_2,n_2} + ju_{k_2,n_2}) \end{aligned} \tag{3.22}$$

Consider a parameter *C* as the ratio between the imaginary and real part of $H^{(c)}_{k_1,n_1}$,i.e.,$H^{(c)}_{k_1,n_1} = H^{(r)}_{k_1,n_1} + jH^{(i)}_{k_1,n_1}$ and $C = H^{(i)}_{k_1,n_1}/H^{(r)}_{k_1,n_1}$. Then taking the real and imaginary parts of each equation in Eq. 3.22, we get

$$\begin{aligned} y^{(r)}_{k_1,n_1} &= H^{(r)}_{K_1,n_1} d_{k_1,n_1} - CH^{(r)}_{k_1,n_1} u_{k_1,n_1} \\ y^{(i)}_{k_1,n_1} &= CH^{(r)}_{K_1,n_1} d_{k_1,n_1} + H^{(r)}_{k_1,n_1} u_{k_1,n_1} \\ y^{(r)}_{k_2,n_2} &= H^{(r)}_{K_2,n_2} d_{k_2,n_2} - CH^{(r)}_{k_2,n_2} u_{k_2,n_2} \\ y^{(i)}_{k_2,n_2} &= CH^{(r)}_{K_2,n_2} d_{k_2,n_2} + H^{(r)}_{k_2,n_2} u_{k_2,n_2} \end{aligned} \tag{3.23}$$

As the channel is invariant we set $H^{(c)}_{k_2,n_2} = H^{(c)}_{k_1,n_1}$ and by a combination of the above equations, we get:

$$\begin{aligned} X1 &= d_{k_2,n_2} y^{(r)}_{k_1,n_1} - d_{k_1,n_1} y^{(r)}_{k_2,n_2} \\ &= CH^{(r)}_{k_1,n_1}(-d_{k_2,n_2} u_{k_1,n_1} + d_{k_1,n_1} u_{k_2,n_2}) \\ X2 &= d_{k_2,n_2} y^{(i)}_{k_1,n_1} - d_{k_1,n_1} y^{(i)}_{k_2,n_2} \\ &= H^{(r)}_{k_1,n_1}(d_{k_2,n_2} u_{k_1,n_1} - d_{k_1,n_1} u_{k_2,n_2}) \end{aligned} \tag{3.24}$$

Then the X_1/X_2 ratio gives:

$$C = \frac{d_{k_2,n_2} y^{(r)}_{k_1,n_1} - d_{k_1,n_1} y^{(r)}_{k_2,n_2}}{d_{k_1,n_1} y^{(i)}_{k_2,n_2} - d_{k_2,n_2} y^{(i)}_{k_1,n_1}} \tag{3.25}$$

Then the first two equations in Eq. 3.23 can be written as:

$$\begin{aligned} y^{(r)}_{k_1,n_1} &= H^{(r)}_{k_1,n_1} d_{k_1,n_1} - CH^{(r)}_{k_1,n_1} u_{k_1,n_1} \\ Cy^{(i)}_{k_1,n_1} &= C^2 H^{(r)}_{k_1,n_1} d_{k_1,n_1} + CH^{(r)}_{k_1,n_1} u_{k_1,n_1} \end{aligned} \tag{3.26}$$

The sum of two above equations gives:

$$H^{(r)}_{k_1,n_1} d_{k_1,n_1}(1 + C^2) = y^{(r)}_{k_1,n_1} + Cy^{(i)}_{k_1,n_1} \tag{3.27}$$

Therefore, the real and imaginary components of the channel are:

$$\begin{aligned} H^{(r)}_{k_1,n_1} &= \frac{y^{(r)}_{k_1,n_1} + C y^{(i)}_{k_1,n_1}}{d_{k_1,n_1}(1+C^2)} \\ H^{(i)}_{k_1,n_1} &= C H^{(r)}_{k_1,n_1} \end{aligned} \tag{3.28}$$

So, channel coefficients are estimated. This method does not require any knowledge of the prototype function,can be used as preamble-based method and also as a scattered based channel estimation method.

CHAPTER 4

FAST CONVOLUTION FILTER BANK STRUCTURE

This chapter focuses on a special implementation scheme for multirate filter banks which is based on fast-convolution (FC) processing. The basic idea of fast convolution is that a high-order filter can be implemented effectively through multiplication in frequency domain, after taking DFT's of the input sequence and the filter impulse response. Eventually, the time-domain output is obtained by IDFT. Commonly, efficient implementation techniques, like FFT/IFFT, are used for the transforms, and overlap-save processing is adopted for processing long sequences.

4.1 Review on Fast Convolution

The convolution theorem tells us that multiplication in the frequency domain is equivalent to convolution in the time domain. Circular convolution is achieved by multiplying two discrete Fourier transforms (DFTs) to effect convolution of the time sequences that the transforms represent. By using the FFT to implement the DFT, the computational complexity of circular convolution is approximately $O(Nlog2N)$ instead of $O(N^2)$, as in direct linear convolution. Although very small FIR filters are most efficiently implemented with direct convolution, fast convolution is the clear winner as the FIR filters get longer.

Fast convolution refers to the blockwise use of circular convolution to accomplish linear convolution. Fast convolution can be accomplished by OA(overlap-Add) or OS(Overlap-save) methods. OS is also known as "overlap- scrap". In OA filtering, each signal data block contains only as many samples as allows circular convolution to be equivalent to linear convolution. The signal data block is zero-padded prior to the FFT to prevent the filter impulse response from "wrapping around" the end of the sequence. OA filtering adds the input-on transient from one block with the input-off transient from the previous block.

In OS filtering, no zero-padding is performed on the input data, thus the circular

convolution is not equivalent to linear convolution. The portions that "wrap around" are useless and discarded. To compensate for this, the last part of the previous input block is used as the beginning of the next block. OS requires no addition of transients, making it faster than OA.

4.2 Synthesis and Analysis filter banks

The structures of FC-based synthesis filter bank(SFB) is shown in Fig. 4.1. In synthesis filter bank, the incoming discrete time input signals $x_k(n)$'s are first transformed to frequency domain using discrete fourier transform. The resulting frequency domain signals are then shifted in frequency domain to their desired positions and weighted such that their spectra do not undesirably overlap. The weighted and shifted frequency-domain subband signals are combined in frequency domain and converted back to the time-domain with the aid of inverse discrete Fourier transform. Then the output of this block is partially removed or added to the block's previous output depending on overlap-Add or overlapp-save method and is transmitted.

The structure of FC-based flexible analysis filter bank (AFB) is illustrated in Fig. 4.2 We consider a case where the incoming high-rate, wideband signal is to be split into several narrowband signals with adjustable frequency responses and adjustable sampling rates. We are interested in cases where the output signals are critically sampled or oversampled by a small factor. We also note that different subbands may be overlapping

Fig. 4.2 includes the sampling reduction by factors

$$R_k = N/L_k = N_s/L_{s,k} \tag{4.1}$$

where *k* is the subband index. The sampling rate conversion factor is determined by the IFFT size, and can be configured for each subband individually. Naturally, the IFFT size determines the maximum number of frequency bins, i.e., the bandwidth of the subband. It is also possible to increase the subband output sampling rate by increasing the IFFT size by adding zero-valued bins outside the wanted subband frequency range. In communication applications, a subband would contain a communication waveform with the specific symbol rate, and the output sampling rate is normally chosen as its

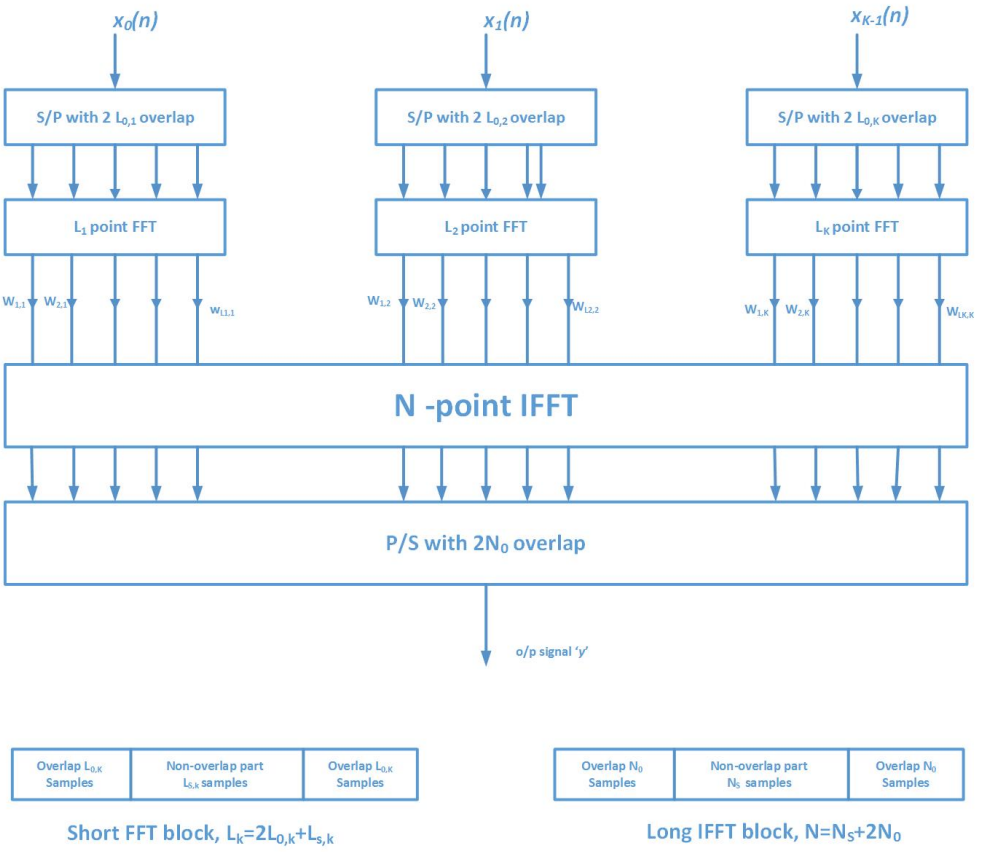

Figure 4.1: Fast convolution based synthesis analysis filter bank using overlap-save processing.

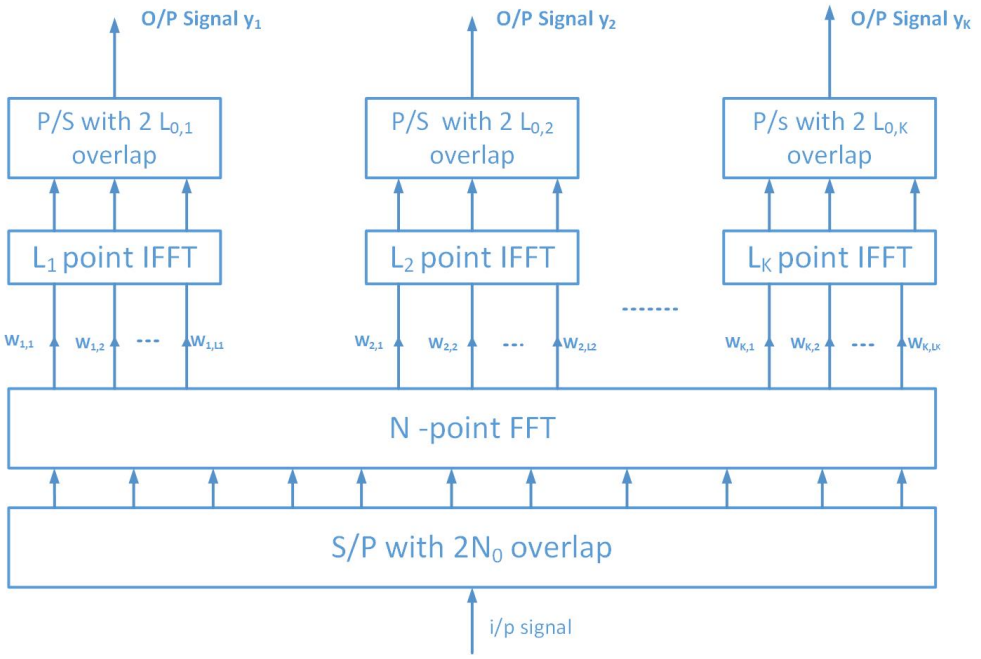

Figure 4.2: Fast convolution based analysis analysis filter bank using overlap-save processing.

(small) integer multiple. Regardless of the specific processing applied for each subband, the decimation factor of the structure of Fig. 4.2 is given by Eq. 4.1. This means that the length of the FC output block is reduced by the same factor, and so is also the length of the overlapping part in the overlap-save processing. The input and output block lengths have to exactly match, taking into account the sampling rate conversion factor.

There are two key parameters which have an effect on the spectral characteristics of the FC-FB scheme:

- The IFFT size L is defining how well the filter frequency response can be optimized. In general, increasing the value of L helps to improve the stopband attenuation.
- The overlap factor $1 - L_s/L$: In FC based multirate signal processing there is an inevitable cyclic distortion effect because the overlapping part of the processing block cannot be made big enough to absorb the tails of the filter impulse response. Naturally, this effect can be reduced by increasing the overlap factor.

The FC-FB model can be used for generating and demodulating different kinds of communication waveforms. In our approach, the basic design is done for a filter channel with roll-off of one. The frequency-domain weights consist of two symmetric transition bands and all stopband bins are set to zero. The subchannel spacing is half of the overall bandwidth, which is equal to the IFFT length. Therefore, the subchannels are oversampled by two, which is also necessary for staggered, OQAM type subchannel processing. OQAM subcarrier signal model, in turn, is necessary for reaching (near) orthogonality of overlapping subcarriers in FB systems.

Filter design

To reach orthogonality in FBMC/OQAM systems, RRC type sub-channel filters are used in synthesis bank of Tx and analysis bank of Rx. Common choice for Roll-off factor is 1. One possible design for RRC and RC type designs, FFT domain weights of filter transition bands can be obtained by readily by sampling half a cycle of the cosine function(RC case) or its square root(RRC case). However this suffers from cyclic distortion and not optimal in any sense.

Optimization principles: We consider cases with the roll-off factor of one and subchannel oversampling factor of two. The IFFT length L is assumed to be even. Then it

foloows that each subband has *L-1* non-zero frequency domain weights. for an example. Only one stopband bin is included in the IFFT and, following strictly the RRC response symmetry, the corresponding weight becomes zero. The center weight (at DC in the lowpass filter case) takes the value 1 and, when *L* is a multiple of four, the two weights in the middle of the transition bands take the value 1/2 for RC cases and $1/\sqrt{2}$ in RRC cases. In the RC case, each pair of weights located symmetrically around in the transition band add up to one, and in the RRC case their squares add up to one. Consequently, in both cases there are [*L*/4]-1 independent parameters in the optimization. These values can be determined by optimization with respect to interference.

4.3 Embedded equalizer

Here a subchannel-wise channel equalization structure was considered where the channelization weights of the fastconvolution filter bank structure are also used for channel equalization purposes. This frequency-domain equalization scheme is referred to as an embedded equalizer. This model approximates closely a linear fractionally spaced equalizer and conceptual model of the receiver front-end invludes the following elements.

- Pulse-shape matched filter: The FC-FB realizes the root raised cosine(RRC) type pulse shape filter through thr weights $w_{k,n}$'s. Here, *n* is the FFT bin index and *k* is subchannel index.
- Channel matched filter $H^*_{k,n}$, where $H_{k,n}$ is the subchannel frequency response at the corresponding FFT bin.
- Folding effect(aliasing) due to resampling at the symbol rate.
- Linear equalizer with mean squared error(MSE) criterion.

The resulting frequency domain weights can be determined as

$$\hat{w}_{k,n} = \frac{H^*_{k,n} w^*_{k,n}}{|H_{k,n} w_{k,n}|^2 + |H_{k,\tilde{n}} w_{k,\tilde{n}}|^2 + 1/\sigma} \tag{4.2}$$

where σ is the signal-to-noise ratio and $\tilde{n}$ is the FFT bin index folding on top of FFT bin *n* in subchannel *k*

CHAPTER 5

SIMULATION RESULTS

5.1 Simulation parameters

The following parameters are used for simulations

- Number of subcarriers,M=512.
- Number of active sub-carriers=390
- Cyclic prefix length,N_{CP}=64.
- Bandwidth of the system,W=20MHz.
- Channel model: Vehicular-A channel
- Roll-off factor, ρ=1
- Overlapping factor,K=4
- SNR range=0 to 30dB
  for FC-FB system:
- small FFT/IFFT size, L=16
- Large FFT/IFFT size, M=512
- Non-overlapping factor, L_s=8,10

5.2 Spectrum comparisons

Fig. 5.1 shows Transmit spectrums of OFDM systems and PPN-FBMC systems. Some null carriers are introduce to show, how much FBMC gives advantage over OFDM in case of sideband suppression.

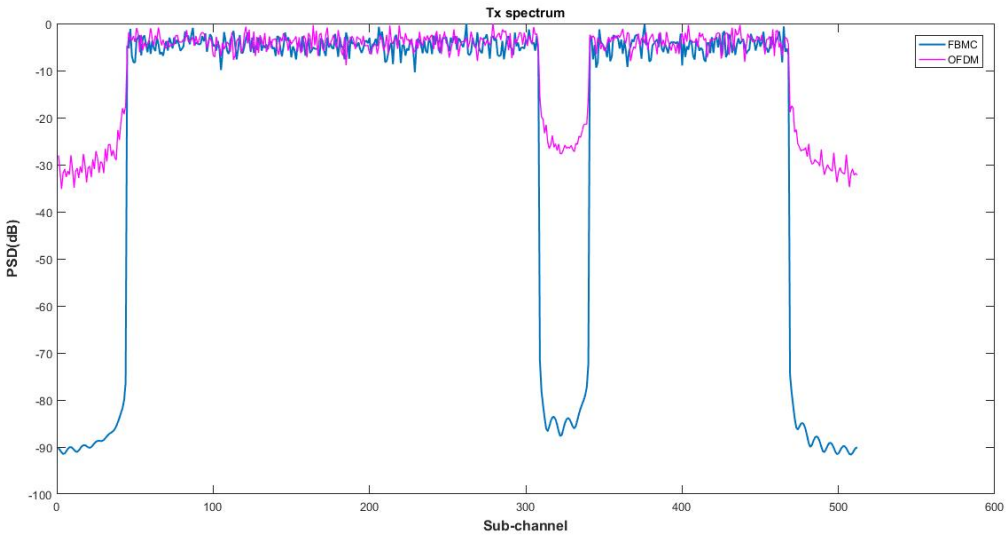

Figure 5.1: OFDM vs FBMC spectrum

Fig. 5.2 shows spectral characteristics of Polyphase and Fast-Convolution structures.

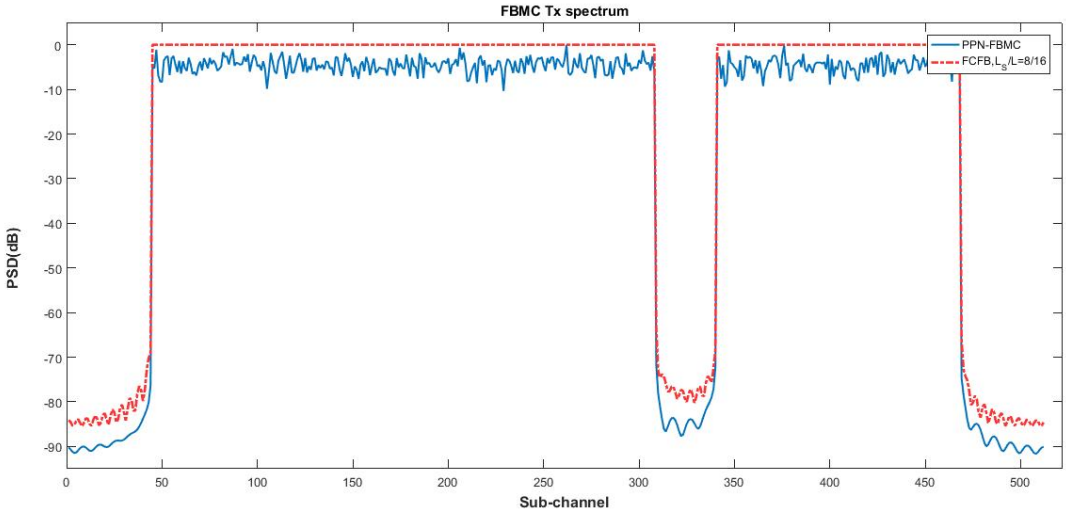

Figure 5.2: FBMC-PPN vs FCFB spectrum

Fig. 5.3 shows FC-FB Tx spectrum for two values of L_s=8 and 10.

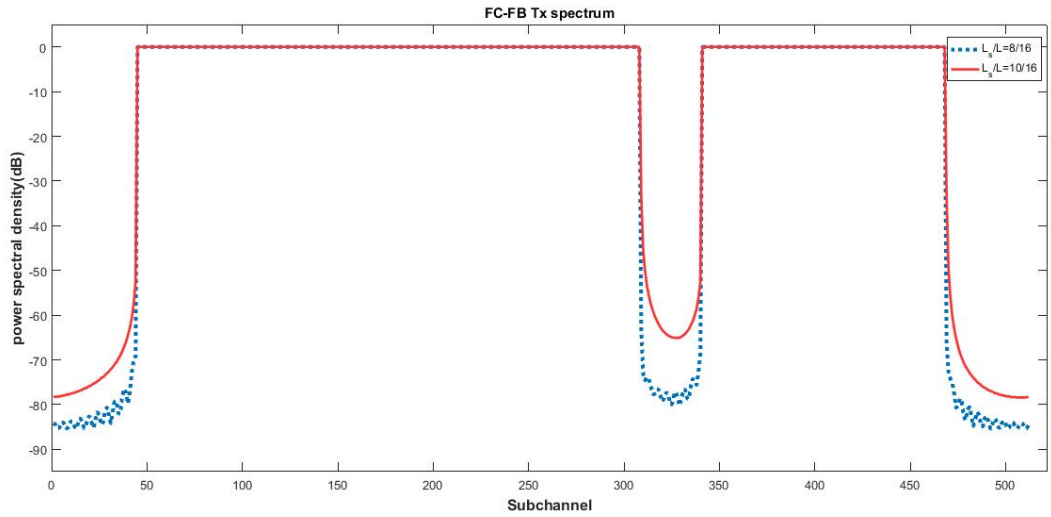

Figure 5.3: FC-FB Tx spectrum for two overlapping factors

5.3 BER comparisons

Fig. 5.4 shows performance over AWGN channel. It shows FBMC system is equivalent to OFDM/QPSK/BPSK system in case of AWGN system.

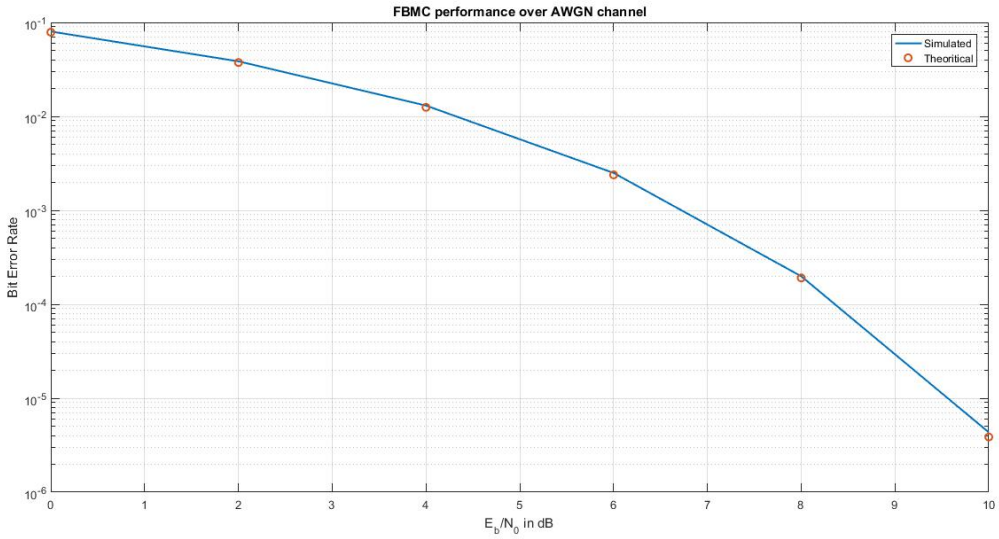

Figure 5.4: FBMC system performance over AWGN channel

Fig. 5.5 shows performance comparison of OFDM system and Polyphase Filter bank structure in Vehicular-A channel with perfect channel information at receiver.

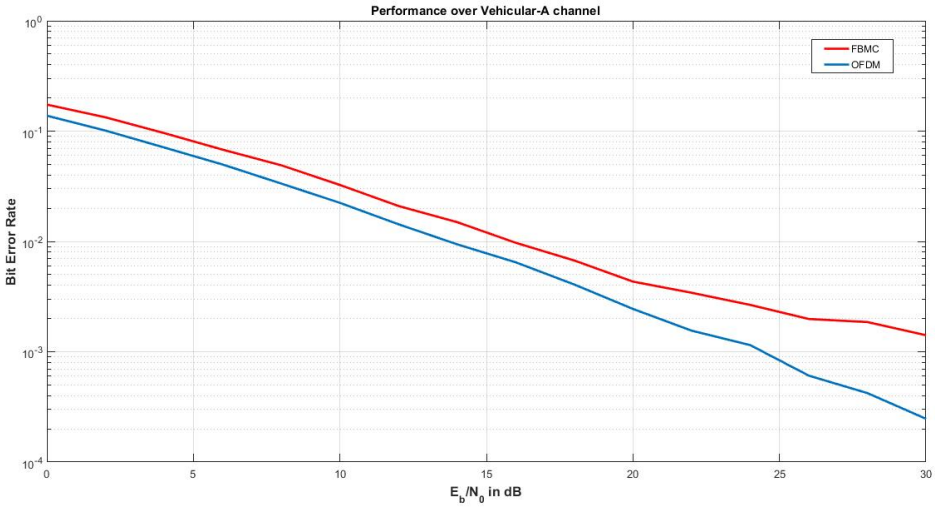

Figure 5.5: BER comparison of OFDM and FBMC systems

Fig. 5.6 shows BER comparisons of FBMC system with different channel estimation techniques in Rayleigh channel(Vehicular-A channel).

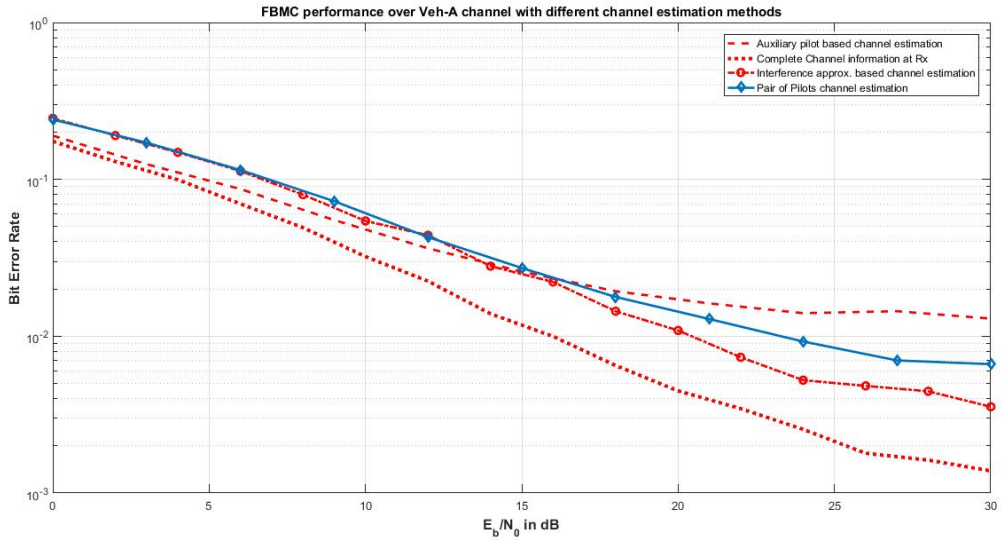

Figure 5.6: Polyphase filter bank performance with channel estimation in Vehicular-A channel

Fig. 5.7 shows BER performance of polyphase structure and fast convolution structures in Vehicular-A channel.

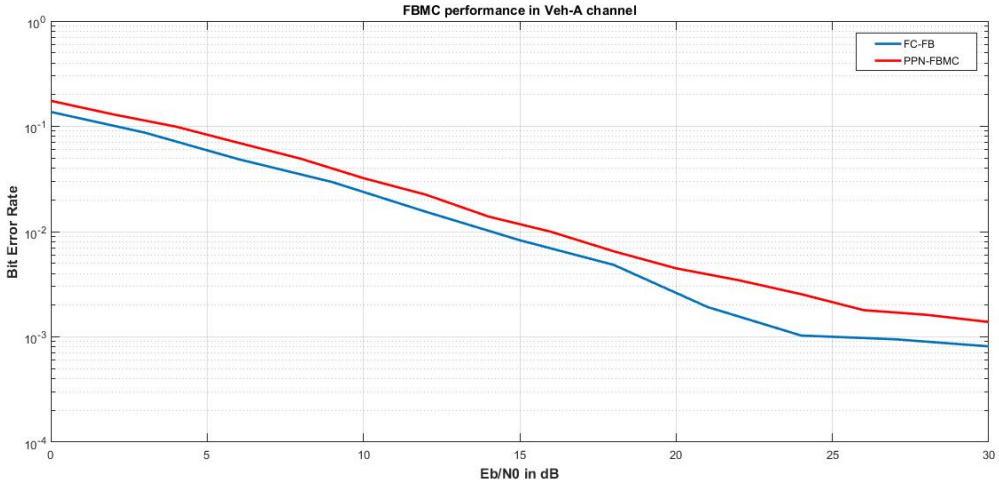

Figure 5.7: Performance comparion between FBMC and FCFB systems

CHAPTER 6

Conclusions and Futurework

Two types of FBMC system implementation are studied. FBMC systems gives advantage over OFDM systems in spectral efficiency and sideband suppression at the cost of slightly higher computational complexity. This makes FBMC better choice for cognitive radios. FC-FB can be used for efficient implementation of FBMC/OQAM, with potential for reduced computational complexity compared to traditional polyphase implementations.

In this project,simple FIR equalizer and preamble based channel estimation techniques are considered.Further work can include Extending these results to scatter based channel estimation techniques and coming with simple MMSE equalizer.

REFERENCES

1. **F. Schaich**, "Filterbank based multi carrier transmission(fbmc)-evolving OFDM:FBMC in the context of wimax.", in Wireless Conference(EW),2010 European, April 2010,pp.1051-1058.

2. **J. Yli-Kaakinen and M. Renfors**, "Fast-convolution filter bank approach for non-contiguous spectrum use," in Proc. Future Network and MobileSummit, Lisbon, Portugal, July 3-5 2013.

3. **M. Renfors, J. Yli-Kaakinen, and f. harris**, "Analysis and design of efficient and flexible fast-convolution based multirate filter banks," submitted to IEEE Trans. Signal Processing, 2013.

4. **M. Borgerding**, "Turning overlap-save into a multiband mixing, downsampling filter bank," IEEE Signal Processing Mag., pp. 158-162, Mar. 2006.

5. **T. Ihalainen, T. H. Stitz, M. Rinne, and M. Renfors**, "Channel equalization in filter bank based multicarrier modulation for wirelesscommunications," EURASIP Journal on Advances in Signal Processing, Article ID 49389, 18 pages, 2007.

6. **T. H. Stitz, T. Ihalainen, A. Viholainen, and M. Renfors**, "Pilot-based synchronization and equalization in filter bank multicarrier communications," EURASIP J. Adv. Signal Process., 2010, Article ID 741429.

7. **C. Lele, J.-P. Javaudin, R. Legouable, A. Skrzypczak, and P.Siohan**, "Channel estimation methods for preamble-based OFDM/OQAM modulations," in Proceedings of the European Wireless Conference, Paris, France, April 2007.

8. FP7-ICT project PHYDYAS- Physical Layer for Dynamic Spectrum Access and Cognitive Radio, http://www.ict-phydyas.org.

9. **K. Shao, J. Alhava, J. Yli-Kaakinen, and M. Renfors**, "Fast-convolution implementation of filter bank multicarrier waveform processing," in IEEE Int. Symp. on Circuits and Systems (ISCAS 2015), Lisbon, Portugal, May 2015.

10. **M. Renfors and J. Yli-Kaakinen**, "Channel equalization in fastconvolution filter bank based receivers for professional mobile radio," in Proc. European Wireless, Barcelona, Spain, May 14-16 2014.

11. **P. P. Vaidyanathan**, Multirate Systems and Filter Banks, Prentice-Hall, Englewood Cliffs, NJ, USA, 1993.